



# Breeze-driven triboelectric nanogenerator for wind energy harvesting and application in smart agriculture

Xiang Li<sup>a,b,1</sup>, Yuying Cao<sup>a,1</sup>, Xin Yu<sup>a,1</sup>, Yuhong Xu<sup>a</sup>, Yanfei Yang<sup>a,b</sup>, Shiming Liu<sup>b</sup>, Tinghai Cheng<sup>a,c,\*</sup>, Zhong Lin Wang<sup>a,c,d,\*</sup>

<sup>a</sup> Beijing Institute of Nanoenergy and Nanosystems, Chinese Academy of Sciences, Beijing 101400, China

<sup>b</sup> School of Mechanical Engineering, Shenyang Jianzhu University, Shenyang, Liaoning 110168, China

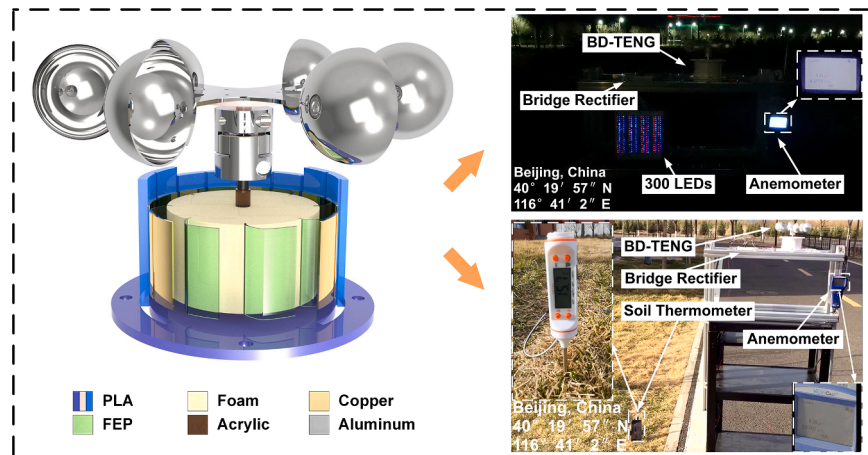
<sup>c</sup> CUSTech Institute of Technology, Wenzhou, Zhejiang 325024, China

<sup>d</sup> School of Materials Science and Engineering, Georgia Institute of Technology, Atlanta, GA 30332-0245, United States

## HIGHLIGHTS

- The breeze-driven triboelectric nanogenerator is proposed.
- The prototype can harvest the breeze energy efficiently.
- The start-up wind speed of the prototype is as low as 3.3 m/s.
- The energy conversion efficiency of the prototype can reach 12.06%.

## GRAPHICAL ABSTRACT



## ARTICLE INFO

### Keywords:

Triboelectric nanogenerator  
Natural breeze  
Energy harvesting  
Smart agriculture

## ABSTRACT

Smart agriculture is becoming an inevitable trend with the wide application of sensor networks. To supply energy for agricultural sensors, the wind energy harvester supports a possible solution. However, the average wind speed on the earth surface is only 3.28 m/s, which cannot easily be harvested by traditional generators efficiently. To efficiently harvest breeze energy in the farmland environment, a breeze-driven triboelectric nanogenerator (BD-TENG) was proposed. By selecting lightweight rotor materials and designing suitable wind scoops structures, the start-up wind speed of BD-TENG is as low as 3.3 m/s, and when the wind speed is 4 m/s, the energy conversion efficiency of the BD-TENG can reach 12.06%. Moreover, under 4 m/s wind speed, the output performance of the BD-TENG is 330 V, 7  $\mu$ A, 137 nC, and the peak power is 2.81 mW. So, the BD-TENG is easier to operate normally even in low wind speed environments and can harvest natural breeze energy efficiently.

\* Corresponding authors.

E-mail addresses: [chengtinghai@binn.cas.cn](mailto:chengtinghai@binn.cas.cn) (T. Cheng), [zhong.wang@mse.gatech.edu](mailto:zhong.wang@mse.gatech.edu) (Z.L. Wang).

<sup>1</sup> These authors contributed equally to this work.

<https://doi.org/10.1016/j.apenergy.2021.117977>

Received 12 May 2021; Received in revised form 22 September 2021; Accepted 27 September 2021

0306-2619/© 2021 Elsevier Ltd. All rights reserved.

Experiments prove that in natural environments, the BD-TENG successfully lights up 300 red and blue light-emitting diodes in series, which can be applied to increase lighting time for plants at night. Moreover, the BD-TENG can power a soil thermometer by harvesting natural breeze energy. Therefore, the BD-TENG can be widely used in farmland environments to provide energy for agricultural sensor networks. The BD-TENG has bright prospects in smart agriculture and can promote its sustainable development.

## Nomenclature

$m$	rotor mass of the BD-TENG
$n$	input speed of the BD-TENG
$E_k$	the kinetic energy of the rotor
$\bar{P}_1$	average input power of the BD-TENG
$S$	total windward area of the wind scoops
$\eta_{\text{avg}}$	average energy conversion efficiency
$J_1$	moment of inertia of the rotor
$T$	input torque of the BD-TENG
$\bar{P}_0$	the average output power of the BD-TENG
$J_2$	moment of inertia of the wind scoop

## 1. Introduction

Agriculture is an important industrial sector that supports the construction and development of the national economy. By combining traditional agriculture and modern science and technology, smart agriculture effectively improves the ability to respond to natural disasters thereby improving agricultural production efficiency [1]. Sensors are widely applied in smart agriculture, such as monitoring and controlling the ambient environment of crops to ensure healthy growth. However, how to meet the energy requirement of sensors is a tricky problem. The traditional power supply method requires laborious manual operation to replace the waste batteries, moreover, the waste batteries might cause environmental pollution [2,3]. In recent years, harvesting the natural mechanical energy in the farmland environment and directly powering agricultural sensors has been considered as the possible approach for solving this problem. Among various mechanical energies, natural wind energy has the advantages of large reserves, wide distribution, renewable, pollution-free, and others. It is an excellent choice to power agricultural sensors by harvesting natural wind energy [4,5]. However, natural wind energy also has limitations of intermittent and instability. For the wind energy generators, when the natural wind speed is lower than the start-up speed, it cannot operate normally or the output will be interrupted. This will affect the efficiency of wind energy harvesting. Therefore, the lower start-up wind speed can make the generator harvest weak wind energy and enhance the operating stability, thus supplying energy for agricultural sensors more stably.

In 2012, based on the coupling effect of contact electrification and electrostatic induction [6–8], Wang's group invented a triboelectric nanogenerator (TENG) for the first time [9]. TENG has many advantages, which include low cost [10], easy manufacturing [11], a wide range of material choices [12], broad application scenarios [13,14], and so forth. It is widely applied to harvest various natural mechanical energy, including ocean energy [15–17], wind energy [18–20], vibration energy [21–23], biomechanical energy [24–26], and sound wave energy [27–28]. Based on the unique power generation characteristics, TENG has an irreplaceable advantage compared with the electromagnetic generators (EMG) in that it has higher low-frequency energy harvest efficiency [29,30]. The EMG is currently the most widely used power generation method and has higher energy conversion efficiency in high-frequency energy environments [31,32]. And the electromagnetic-triboelectric hybrid generator can effectively harvest wide-frequency

wind energy [33,34]. However, the goal of this work is to harvest the breeze energy and supply energy for agricultural sensors. The average wind speed on the earth surface is only 3.28 m/s [35], so the farmland environment is a typical breeze environment. Therefore, the TENG should be chosen to efficiently harvest the breeze energy in the farmland environment.

In recent years, several wind-driven TENG has been developed to be applied in the specific environment of farmland. A fur-brush TENG with a start-up wind speed of 8 m/s was reported to harvest wind energy with high output performance in a high humidity environment by using high humidity resistance animal fur as the dielectric layer [36]. A contactless mode triggering-based ultra-robust rotary hybridized nanogenerator was reported with a low wind speed of 2 m/s [37]. The output power of TENG is about 5.39 mW with an input speed of 500 r/min. These previous works are of great significance to promote the wide application of the TENG in smart agriculture, but they do not have the two advantages of low start-up wind speed and high energy conversion efficiency. The TENG with the film flutter will be easier to meet these two needs at the same time [19,38]. However, the air inlet and outlet will cause the power generation part to directly contact the external environment, which will seriously affect the output performance and service life of the TENG. Therefore, a sealed TENG structure with low start-up wind speed and high energy conversion efficiency should be designed to effectively harvest the breeze energy in the farmland environment.

In this paper, a breeze-driven triboelectric nanogenerator (BD-TENG) was proposed, which can supply power for sensors by harvesting natural breeze energy in smart agriculture. By choosing low-density materials to make the rotor, the kinetic energy loss and friction loss of the BD-TENG during operation can be reduced, thereby increasing the energy conversion efficiency up to 12.06%. By reducing the mass of the rotor to reduce the moment of inertia, and choosing a suitable wind scoop structure to effectively harvest wind energy can effectively reduce the start-up wind speed, so the starting wind speed of BD-TENG is as low as 3.3 m/s. Moreover, under 4 m/s wind speed, the output performance of the BD-TENG is 330 V, 7  $\mu$ A, 137 nC, and the peak power is 2.81 mW. Therefore, the BD-TENG can operate normally at low wind speeds and harvest the breeze energy efficiently. As a demonstration, based on the low start-up wind speed, the BD-TENG can be driven by the human blowing and power the light-emitting diode board with the pattern "BINN TENG". In natural environments, the BD-TENG can power 300 red and blue light-emitting diodes in series applied to supplement night lighting for crops. Besides, it can successfully power a soil thermometer after a period of natural breeze energy harvesting. Based on the above application experiments, proving the BD-TENG can be widely applied in farmland environments, and power the sensor network required for smart agriculture through harvesting breeze energy. Therefore, the BD-TENG could play a vital role in developing smart agriculture and could promote its sustainable progress.

## 2. Results and discussion

### 2.1. Structural design and operation principle

In smart agriculture, three necessary elements to ensure the normal growth of plants are suitable temperature, humidity, and light intensity, as shown in Fig. 1a. To provide energy for the smart agricultural production system, a breeze-driven triboelectric nanogenerator was designed (BD-TENG) that can effectively harvest the natural breeze energy. Because the wind speed on the earth surface is only 3.28 m/s,

the breeze energy is widely distributed in the farmland. Taking the main grain-producing areas of China as an example, over 90% of days in a year exit an average daily wind speed of lower than 5 m/s (Fig. S1, Supporting Information), which provides bright prospects to the BD-TENG in smart agriculture. Fig. 1b shows the detailed structure of the BD-TENG, which consists of wind scoops, coupling, rotor, stator, and shells. Fig. 1c is the BD-TENG photo, and the photo of the stator structure is shown in Fig. 1d. In addition, the rotor structure photo is depicted in Fig. 1e, which consists of an acrylic shaft, a foamed flywheel, and the FEP films. The natural wind is harvested by the wind scoops, which drives the FEP films to produce sliding friction with the copper electrodes. Therefore, the BD-TENG realizes the conversion of natural wind energy into electric energy.

Fig. 2 shows the power generation principle of the BD-TENG. The four working states during the power generation process are shown in Fig. 2a. The FEP film is an electronegative material, and the copper is an electropositive material. When they contact each other, electrons on the copper-1 surface are transferred to the surface of FEP film based on the triboelectrification principle. [Fig. 2a(i)]. In Fig. 2a(ii), the FEP film gradually slides to copper-2. During this process, electrons are transferred from the copper-2 surface to copper-1, an opposite direction current is generated in the external circuit. As shown in Fig. 2a(iii), the FEP film is completely attached to copper-2, electrons on the copper-2 surface are completely transferred. As described in Fig. 2a(iv), when the FEP film gradually slides to copper-1, electrons on the copper-1 surface are transferred to the copper-2 surface, an opposite direction current is generated in the external circuit. When the FEP film separates from copper-2 again, an electron transferred cycle is completed.

The COMSOL Multiphysics 5.5a software is applied to show changing process of the potential difference (Fig. 2b). The surface charge densities of copper electrodes and FEP films are  $2.54 \text{ nC/cm}^2$  (Eq. S1, Supporting Information). When the FEP film is completely attached to copper-1, Fig. 2b(i) shows the potential difference of the BD-TENG, which reaches the maximum value. When the FEP film gradually slid to copper-2,

the potential difference gradually decreases [Fig. 2b(ii)]. The potential difference increases to the maximum again [Fig. 2b(iii)] when the FEP film is completely attached to copper-2. When the FEP film is gradually slid to copper-1, the potential difference gradually decreases again [Fig. 2b(iv)]. The changing process of the potential difference proves the feasibility of the power generation principle.

## 2.2. Performance

In order to improve the efficiency of harvesting wind energy of the BD-TENG, the experiment is carried out to research the influence of the rotor mass on energy conversion efficiency with different input speeds (Fig. 3). Five input speeds and nine rotor masses have been selected for experiments. The output performance of BD-TENG with the input speed of 100 r/min is shown in Fig. 3a and Fig. S2 (Supporting Information), and the output performances with input speeds of 300 r/min, 500 r/min, 700 r/min, and 900 r/min are described in Fig. S3a-d, respectively (Supporting Information). As shown, when the input speed is constant, the output performance of the BD-TENG will not be affected by variations in rotor mass. However, when the rotor mass remains unchanged, the open-circuit voltage and the transferred charge remain constant as the input speed increases. In addition, the short-circuit current and the load current through the 100-M $\Omega$  resistance increase.

As shown in Fig. 3b and c, the moment of inertia  $J$  and the kinetic energy  $E_k$  of the rotor will increase with the rotor mass  $m$  rising. In addition, the increase of input speed  $n$  will also cause an increase in the kinetic energy  $E_k$ . In natural environments, the wind speed is unstable, which will cause the rotor speed to change frequently. Therefore, the loss of kinetic energy caused by variations in rotor speed can be reduced by adopting a lightweight rotor.

The increase of the rotor mass will cause the increase of the friction of the transmission parts, and the increase of the input speed will cause the increase of the friction between the FEP film and the copper electrode. Both will cause an increase in input torque  $T$  of the BD-TENG. To

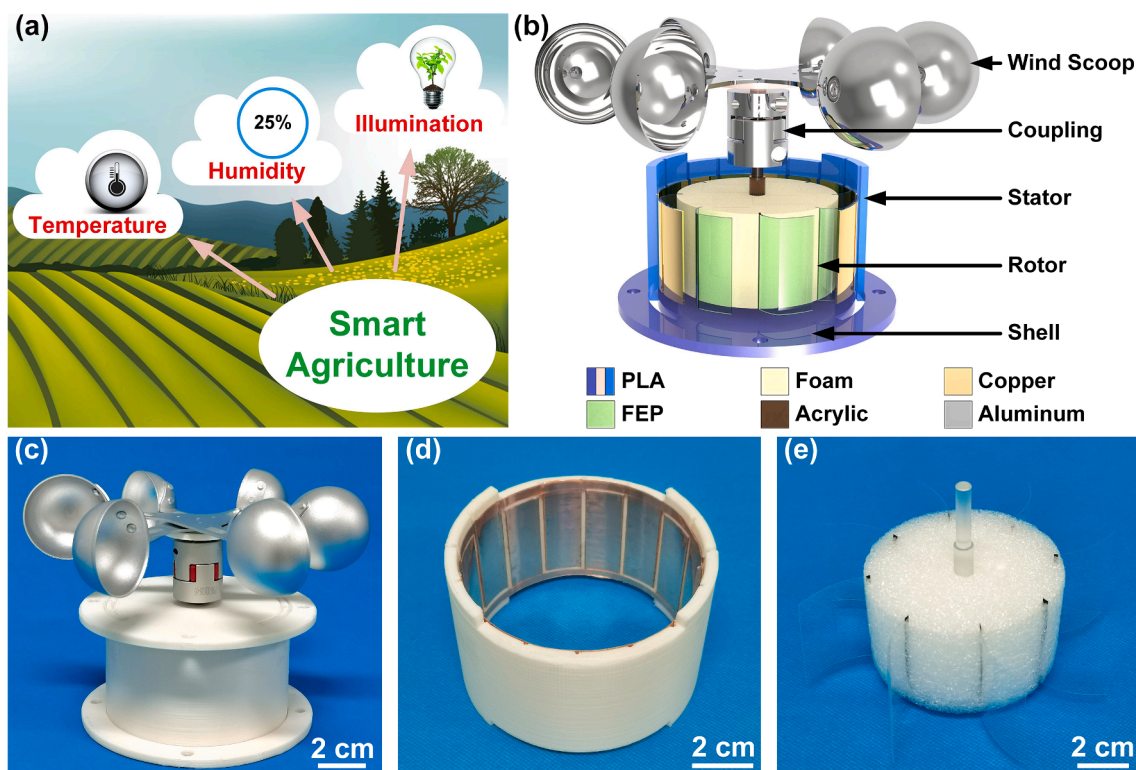


Fig. 1. Structure of the breeze-driven triboelectric nanogenerator (BD-TENG): (a) three essential elements in smart agriculture, (b) illustration of the BD-TENG structure; Photographs of (c) BD-TENG, (d) stator structure, and (e) rotor structure.

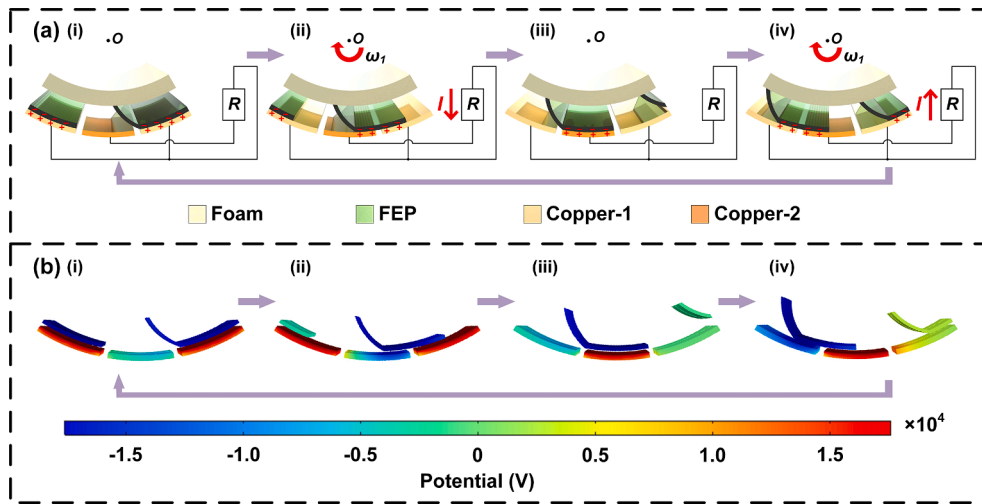


Fig. 2. Power generation principle of the BD-TENG: (a) four working states in the process of power generation, (b) potential simulation diagrams of four working states.

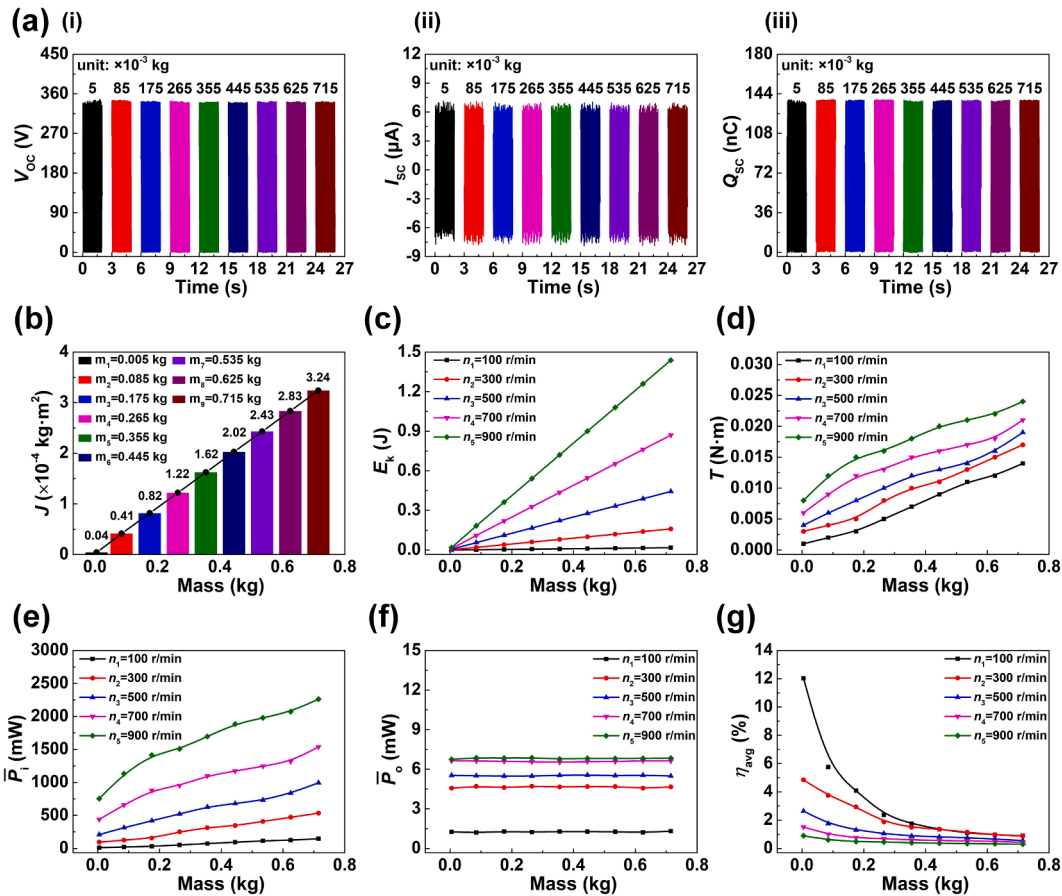


Fig. 3. Influence of the rotor mass on the BD-TENG output performance with different input speeds: (a) the input speed is 100 r/min, (b) moment of inertia  $J$  of different rotors, (c) kinetic energy  $E_k$  of different rotors (d) input torque  $T$ , (e) average input power  $\bar{P}_i$ , (f) average output power  $\bar{P}_o$ , and (g) energy conversion efficiency  $\eta_{avg}$ .

accurately measure the input torque of the generator, a test system is constructed. The stepper motor is used as the excitation source, and the input torque of the excitation source to the BD-TENG is accurately measured through the torque sensor, as shown in Fig. 3d. According to Eq. (1), the average input power  $\bar{P}_i$  of the BD-TENG can be derived as:

$$\bar{P}_i = \frac{Tn}{9549} \quad (1)$$

After calculation, the average input power  $\bar{P}_i$  is shown in Fig. 3e.

According to Eq. (2), the average output power  $\bar{P}_o$  of the BD-TENG can be derived as:

$$\overline{P}_o = \overline{I}_R^2 R, \quad (2)$$

where  $I_R$  is the load current through the external resistance of 100 M $\Omega$ , and  $R$  is the external resistance of 100 M $\Omega$ . After calculation, the average input power  $\overline{P}_i$  is shown in Fig. 3f.

According to Eq. (3), the average energy conversion efficiency  $\eta_{\text{avg}}$  of the BD-TENG can be derived as:

$$\eta_{\text{avg}} = \frac{\overline{P}_o}{\overline{P}_i}. \quad (3)$$

Analysis shows, at the same input speed, the average input power increases linearly with the increase of the input rotor mass. And there is no relationship between rotor mass and output power, the output power of the BD-TENG remains unchanged when the input rotor mass increases. Therefore, when the input speed is the same, the average energy conversion efficiency of the BD-TENG is continuously reduced with the increase of the input rotor mass. On the other hand, when the rotor mass remains constant, as the input speed increases, the average input power of the BD-TENG increases linearly, while the output power increase rate gradually decreases. Therefore, when the rotor mass is the same, as the input speed increases, the average energy conversion efficiency of the BD-TENG continues to decrease. The improvement of average energy conversion efficiency can be achieved by reducing the rotor mass and the input speed (Fig. 3g). The detailed data in Fig. 3g are shown in Tables S1 (Supporting Information).

By choosing lightweight materials, the mass of the rotor could be reduced, and the energy conversion efficiency could be improved. As shown in Table 1, because the density of foam materials is low, the rotor with the foam flywheel has a lower mass of 0.005 kg. When the input speed is 100 r/min, and the rotor mass is 0.005 kg, the average input power, average output power, and average energy conversion efficiency of the BD-TENG are 10.47 mW, 1.263 mW, and 12.06%, respectively. The peak output power and peak energy conversion efficiency of the BD-TENG are 2.81mW and 26.84%, respectively (Fig. S4). In addition, in order to verify the output performance of the BD-TENG when the rotor mass is less than 0.005 kg, related experiments are carried out (Fig. S5 and S6). After comparison, the 0.005 kg foam rotor is chosen to be installed in the BD-TENG. For detailed analysis, please refer to Supporting Information.

Furthermore, to study the influence of the rotor mass and input speed on the BD-TENG, the influence of the wind scoops structure on the output performance is also carried out. Fig. 4a and Fig. S7a (Supporting Information) show the BD-TENG output performance with three wind scoops of 50-mm diameter, Fig. 4b and Fig. S7b (Supporting Information) show it with three wind scoops of 80-mm diameter, and Fig. 4c and Fig. S7c (Supporting Information) show it with six wind scoops of 50-mm diameter. As the wind speed increases, the open-circuit voltage and the transferred charge remain unchangeable. However, the short-circuit current and the load current through 100-M $\Omega$  resistance increase.

Fig. 4d shows the influence of the rotor mass on the start-up wind speed of the BD-TENG with different kinds of wind scoops. With the same type of wind scoop, as the rotor mass increases, the start-up wind speed of the BD-TENG increases. Because as the rotor mass increases, the moment of inertia of the rotor increases (Fig. 3b), which makes the BD-TENG is more difficult to start under the breeze environment. On the other hand, the BD-TENG with three wind scoops of 80-mm diameter is the easiest to operate normally under the breeze environment, the start-up wind speed is 2.5 m/s. Secondly, the BD-TENG with six wind scoops of 50-mm diameter also has a lower start-up wind speed of 3.3 m/s. The

**Table 1**  
Densities of different materials in the rotor structure.

	Acrylic	Foam	FEP
$\rho$ (kg/m <sup>3</sup> )	1190	119	2150

reason of which is that the start-up wind speed will decrease with the increase of the total windward area  $S$  of the wind scoops, and after calculation, the total windward area  $S$  of the three types of wind scoops is shown in Table 2.

The relationship between the wind speed and the rotation speed of the BD-TENG with three kinds of wind scoops is shown in Fig. 4e. The start-up wind speed of the BD-TENG with three wind scoops is 2.5 m/s. However, after the wind speed reaches 4 m/s, the rotation speed is lower than the BD-TENG with six wind scoops of 50-mm diameter. Because both the mass and diameter 80-mm diameter scoops are the largest among three kinds of wind scoops, the moment of inertia  $J_2$  is the largest, thus, the rotation speed is slower in a high wind speed environment. The moment of inertia of three kinds of wind scoops is shown in Table 2, and the specific calculation process is shown in the Supporting Information. Because the average output power  $\overline{P}_o$  is proportional to the wind speed, after the wind speed reaches 4 m/s, the BD-TENG with six wind scoops of 50-mm diameter has the highest average output power, as shown in Fig. 4f. Finally, six wind scoops of 50-mm diameter are selected for the BD-TENG to harvest breeze energy. Therefore, BD-TENG has a low start-up wind speed of 3.3 m/s, and when the wind speed is 4 m/s, the energy conversion efficiency can reach 12.06%.

The start-up wind speed of 3.3 m/s is roughly the same as the average wind speed on the earth surface, which enables the BD-TENG to be applied in the breeze environment of farmland appropriately. Taking farmland environments of China as an example, the grain productions of various provinces in 2019 are statistically analyzed (Relevant grain production data can be queried at the official website of the National Bureau of Statistics, <http://www.stats.gov.cn>). The top eight provinces and their grain productions are shown in Fig. S8a and Fig. S9a (Supporting Information). Furthermore, the China Surface Climate Standard Data Set can be queried at the China Meteorological Data Service Center (<http://data.cma.cn>). It is found that, for the representative city of these eight provinces, the monthly average wind speeds are lower than 5 m/s in general (Fig. S8b-i and Fig. S9b-i, Supporting Information), which is a typical breeze environment. This proves that the BD-TENG is meaningful in the farmland environment.

### 2.3. Demonstration

The peak power with different resistances of the BD-TENG at various input speeds is measured (Fig. 5a). And it is 0.58 mW, 2.81 mW, 5.59 mW, 9.74 mW, 12.51 mW, and 14.76 mW, respectively, when the load resistance is 100 M $\Omega$ . When the input speed is 100 rpm, the charging performance of the BD-TENG for seven commercial capacitors is shown in Fig. 5b, and the BD-TENG can charge a 10  $\mu$ F capacitor to 12 V in 38 s. The load voltage and the load current of the BD-TENG are shown in Fig. 5c.

As shown in Fig. 5d, because the BD-TENG has a lower start-up wind speed, it can be driven by an adult man blowing into the wind scoops to supply power to the light-emitting diode board with the pattern "BINN TENG" (Movie S1, Supporting Information). This proves that the BD-TENG can be well applied in the typical breeze environment of farmland. As shown in Fig. 5e, in natural environments, the BD-TENG can harvest natural breeze energy to supply power to 300 red and blue light-emitting diodes in series, which can supplement lighting for plants at night and promote the growth of crops (Movie S2, Supporting Information). This extra light will increase the blue and red wavelengths of lighting for plants, which has a significant effect on plant growth. Besides, As shown in Fig. 5f, the BD-TENG can drive an agricultural thermometer to operate normally by harvesting the breeze energy in the natural environment to monitor the temperature of the soil where crops are grown (Movie S3, Supporting Information). Therefore, the BD-TENG can normally power some small agricultural sensors, which is of great significance for monitoring crop growth environment information and

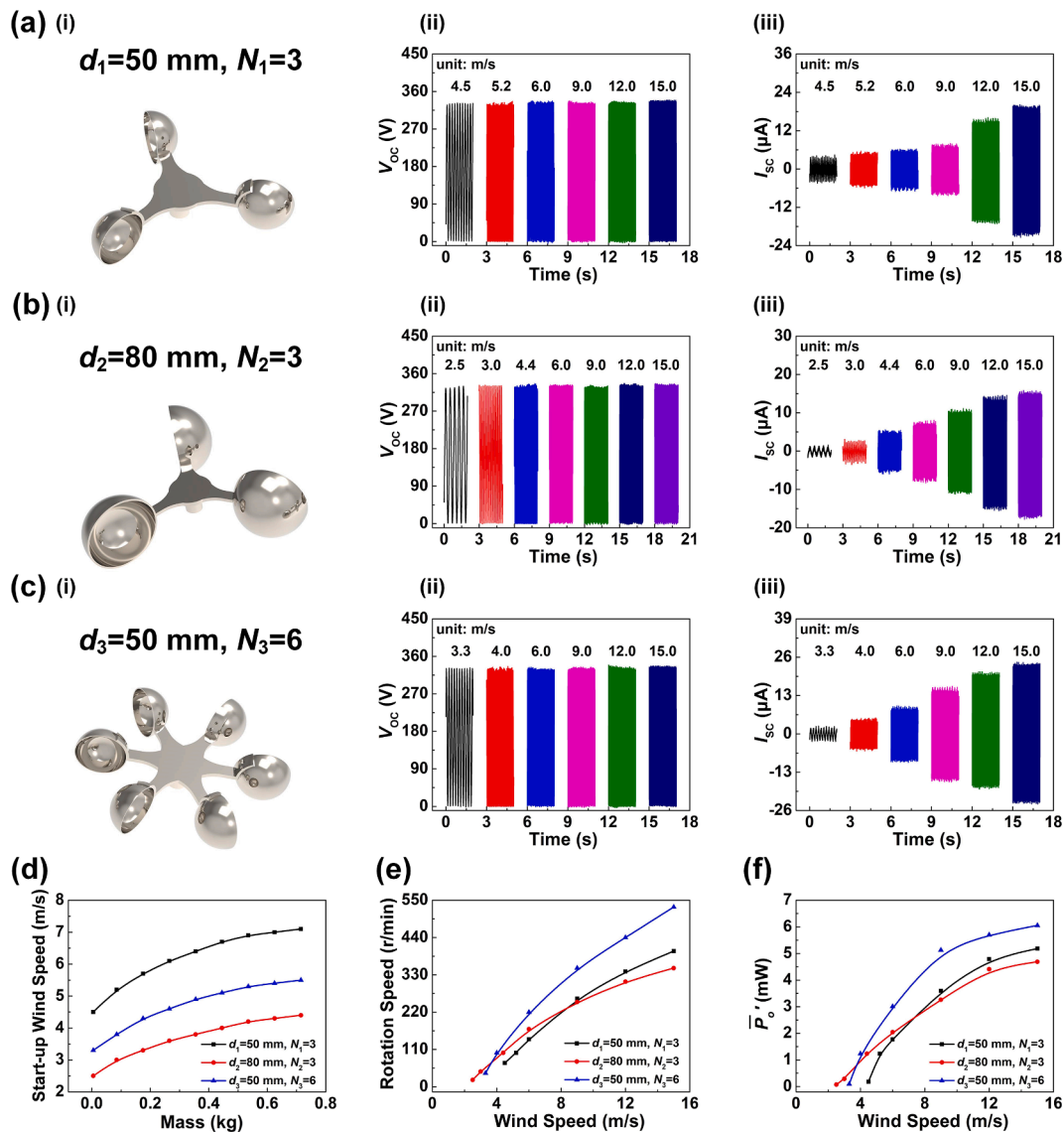


Fig. 4. The output performance of the BD-TENG with three kinds of wind scoops: (a) three wind scoops of 50-mm diameter, (b) three wind scoops of 80-mm diameter, and (c) six wind scoops of 50-mm diameter; Performance comparison of the BD-TENG with different wind scoops structures: (d) start-up wind speed with different rotor mass, (e) relationship between wind speed and rotation speed, and (f) average output power  $\overline{P}_o$  at different wind speeds.

Table 2  
The total windward area  $S$  and moment of inertia  $J_2$  of three kinds of wind scoops.

	$d_1 = 50 \text{ mm}, N_1 = 3$	$d_2 = 80 \text{ mm}, N_2 = 3$	$d_3 = 50 \text{ mm}, N_3 = 6$
$S \text{ (m}^2\text{)}$	0.01178	0.02356	0.03015
$J_2 \text{ (kg}\cdot\text{m}^2\text{)}$	$2.17 \times 10^{-4}$	$9.14 \times 10^{-4}$	$4.34 \times 10^{-4}$

ensuring crop growth.

To better apply the BD-TENG in the actual environment of farmland, it uses the shell to seal the generation, reducing the negative impact of the external environment on the output performance. To verify the sealing effect of the shell, the influence of different humidity environments on the output performance of the BD-TENG is researched, as shown in Fig. S10. In a high-humidity environment, the BD-TENG with a sealed shell has better output performance than directly exposing the generation unit to the outside environment. To verify that the BD-TENG can operate stably for a long time, a long-term operation experiment was carried out under a normal temperature and humidity environment. As shown in Fig. S11, during the 100,000 cycles of the BD-TENG operation,

the open-circuit voltage is relatively stable, and the total attenuation rate is 5%. This proves that the BD-TENG can be used as a stable power source to supply energy for agricultural sensor networks by harvesting natural breeze energy and has important guiding significance for the development of smart agriculture.

### 3. Conclusions

In summary, the wind speed of major grain-producing provinces in China was summarized, and the statistics prove that the natural wind in the farmland environment is low frequency typically. Therefore, a breeze-driven triboelectric nanogenerator (BD-TENG) was designed, which is applied in smart agriculture to harvest natural breeze energy efficiently and provide energy for agriculture sensors. By selecting lightweight rotor materials and designing a suitable wind scoops structure, the start-up wind speed of the BD-TENG could be as low as 3.3 m/s, and the energy conversion efficiency of the BD-TENG could reach 12.06% with the wind speed of 4 m/s. Therefore, the BD-TENG can operate normally in a low wind speed environment and harvest breeze energy efficiently. When the input speed is 100 rpm, the peak power of

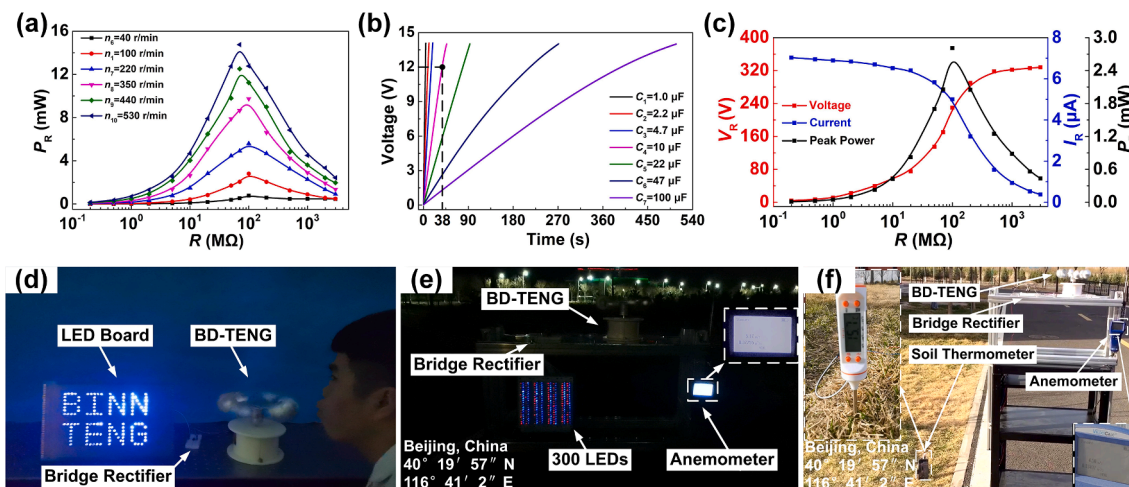


**Fig. 5.** Performance demonstration of the BD-TENG: (a) peak power with different input speeds of the BD-TENG, (b) charging performance of the BD-TENG for five capacitors, (c) load voltage, load current and the peak power, (d) BD-TENG can be driven by the human blowing, (e) BD-TENG can power 300 red and blue light-emitting diodes in series, and (f) BD-TENG can harvest natural breeze energy to power a soil thermometer.

the BD-TENG is 2.81 mW, and which can charge a 10  $\mu\text{F}$  capacitor to 12 V in 38 s. In natural environments, the BD-TENG can harvest natural breeze energy to light up 300 light-emitting diodes in series used to supplement lighting for plants at night. Besides, it can successfully power the soil thermometer by harvesting breeze energy. Therefore, the BD-TENG has bright prospects in smart agriculture and can promote the sustainable development of smart agriculture.

## 4. Experimental section

### 4.1. Fabrication of the BD-TENG

The external dimensions of the breeze-driven triboelectric nanogenerator (BD-TENG) are 200 mm (diameter)  $\times$  140 mm (height). The main structure of the BD-TENG includes the wind scoops, coupling, stator, rotor, and shell. The material of the wind scoops and the coupling is aluminum alloy. The stator and shell are made from polylactic acid (PLA) using a 3D printer (A6S, JGAURORA, P. R. China). Sixteen copper electrodes are evenly fixed on the inner wall of the stator, which dimensions are 40 mm (length)  $\times$  17 mm (width)  $\times$  65  $\mu\text{m}$  (thickness). The rotor is composed of the shaft, flywheel, and fluorinated ethylene propylene (FEP) films. The material of the shaft is acrylic, which is made by turning. The material of the flywheel is foam, which dimensions are 80 mm (diameter)  $\times$  40 mm (height). The dimensions of eight fluorinated ethylene propylene (FEP) films are 40 mm (length)  $\times$  35 mm (width)  $\times$  100  $\mu\text{m}$  (thickness). Please see the [Supporting Information](#) for other information.

### 4.2. Electrical measurement

In order to test the performance of the BD-TENG, the stepper motor (57BYGH56D8EIS-P, HOHI, China) is applied to provides input torque to the BD-TENG. The input torque and rotation speed are measured by the torque sensor (DR-2112-R, Lorenz Messtechnik, Germany). The electrometer (6514, Keithley, USA) is applied to collect electric signals of the BD-TENG, which is converted into data by an acquisition system (BNC-2120, National Instruments, USA). Related data is displayed and stored by the software LabVIEW with the computer. The COMSOL Multiphysics 5.5a software is applied to show changing process of the potential difference.

### CRedit authorship contribution statement

**Xiang Li:** Conceptualization, Investigation, Writing – original draft.

**Yuying Cao:** Investigation, Writing – original draft, Validation. **Xin Yu:** Investigation, Validation. **Yuhong Xu:** Investigation. **Yanfei Yang:** Validation. **Shiming Liu:** . **Tinghai Cheng:** Conceptualization, Resources, Writing – review & editing, Supervision. **Zhong Lin Wang:** Conceptualization, Resources, Writing – review & editing, Supervision.

### Declaration of Competing Interest

The authors declare that they have no known competing financial interests or personal relationships that could have appeared to influence the work reported in this paper.

### Acknowledgements

The authors are grateful for the supports received from the National Key R&D Project from the Minister of Science and Technology (Nos. 2016YFA0202701 and 2016YFA0202704) and the Beijing Municipal Science and Technology Commission (No. Z171100002017017).

### Appendix A. Supplementary material

Supplementary data to this article can be found online at <https://doi.org/10.1016/j.apenergy.2021.117977>.

### References

- [1] Wolfert S, Ge L, Verdouw C, Bogaardt M-J. Big data in smart farming – a review. *Agric Syst* 2017;153:69–80. <https://doi.org/10.1016/j.agry.2017.01.023>.
- [2] Liu J, Chai Y, Xiang Y, Zhang X, Gou Si, Liu Y. Clean energy consumption of power systems towards smart agriculture: roadmap, bottlenecks and technologies. *CSEE J Power Energy* 2018;4(3):273–82.
- [3] Khandelwal G, Chandrasekhar A, Alluri NR, Vivekananthan V, Maria Joseph Raj NP, Kim S-J. Trash to energy: a facile, robust and cheap approach for mitigating environment pollutant using household triboelectric nanogenerator. *Appl Energy* 2018;219:338–49. <https://doi.org/10.1016/j.apenergy.2018.03.031>.
- [4] Adesipo A, Fadeyi O, Kuca K, Krejcar O, Maresova P, Selamat A, et al. Smart and climate-smart agricultural trends as core aspects of smart village functions. *Sensors* 2020;20(21):5977. <https://doi.org/10.3390/s20215977>.
- [5] Gupta M, Abdelsalam M, Khorsandroo S, Mittal S. Security and privacy in smart farming: challenges and opportunities. *IEEE Access* 2020;8:34564–84. <https://doi.org/10.1109/Access.628763910.1109/ACCESS.2020.2975142>.
- [6] Wang ZL, Wang AC. On the origin of contact-electrification. *Mater Today* 2019;30:34–51. <https://doi.org/10.1016/j.mattod.2019.05.016>.
- [7] Zou HY, Zhang Y, Guo LT, Wang PH, He X, Dai GZ, et al. Quantifying the triboelectric series. *Nat. Commun* 2019;10:1427. <https://doi.org/10.1038/s41467-019-09461-x>.
- [8] Wang ZL. On the first principle theory of nanogenerators from Maxwell's equations. *Nano Energy* 2020;68:104272. <https://doi.org/10.1016/j.nanoen.2019.104272>.

- [9] Fan F-R, Tian Z-Q, Lin Wang Z. Flexible triboelectric generator. *Nano Energy* 2012; 1(2):328–34. <https://doi.org/10.1016/j.nanoen.2012.01.004>.
- [10] Wang ZL. Triboelectric nanogenerators as new energy technology and self-powered sensors – principles, problems and perspectives. *Faraday Discuss* 2014;176:447–58. <https://doi.org/10.1039/c4fd000159a>.
- [11] Niu SM, Wang ZL. Theoretical systems of triboelectric nanogenerators. *Nano Energy* 2015;14:161–92. <https://doi.org/10.1016/j.nanoen.2014.11.034>.
- [12] Zhai C, Chou X, He J, Song L, Zhang Z, Wen T, et al. An electrostatic discharge based needle-to-needle booster for dramatic performance enhancement of triboelectric nanogenerators. *Appl Energy* 2018;231:1346–53. <https://doi.org/10.1016/j.apenergy.2018.09.120>.
- [13] Liu Di, Chen B, An J, Li C, Liu G, Shao J, et al. Wind-driven self-powered wireless environmental sensors for Internet of Things at long distance. *Nano Energy* 2020; 73:104819. <https://doi.org/10.1016/j.nanoen.2020.104819>.
- [14] Chen X, Ma X, Ren W, Gao L, Lu S, Tong D, et al. A triboelectric nanogenerator exploiting the bernoulli effect for scavenging wind energy. *Cell Reports Physical* 2020;1(9):100207. <https://doi.org/10.1016/j.xcrp.2020.100207>.
- [15] Yin M, Yu Y, Wang Y, Wang Z, Lu X, Cheng T, et al. Multi-plate structured triboelectric nanogenerator based on cycloidal displacement for harvesting hydroenergy. *Extrem Mech Lett* 2019;33:100576. <https://doi.org/10.1016/j.eml.2019.100576>.
- [16] Jiang T, Pang H, An J, Lu P, Feng Y, Liang Xi, et al. Robust swing-structured triboelectric nanogenerator for efficient blue energy harvesting. *Adv Energy Mater* 2020;10(23):2000064. <https://doi.org/10.1002/aenm.v10.2310.1002/aenm.202000064>.
- [17] Yin M, Lu X, Qiao G, Xu Y, Wang Y, Cheng T, et al. Mechanical regulation triboelectric nanogenerator with controllable output performance for random energy harvesting. *Adv Energy Mater* 2020;10(22):2000627. <https://doi.org/10.1002/aenm.v10.2210.1002/aenm.202000627>.
- [18] Ren Z, Wang Z, Wang F, Li S, Wang ZL. Vibration behavior and excitation mechanism of ultra-stretchable triboelectric nanogenerator for wind energy harvesting. *Extrem Mech Lett* 2021;45:101285. <https://doi.org/10.1016/j.eml.2021.101285>.
- [19] Ren ZW, Wang ZM, Liu ZR, Wang LF, Guo HY, Li LL, et al. Energy harvesting from breeze wind (0.7–6 m s<sup>-1</sup>) using ultra-stretchable triboelectric nanogenerator. *Adv. Energy Mater.* 2020;10:2001770. <https://doi.org/10.1002/aenm.202001770>.
- [20] Lin H, He M, Jing Q, Yang W, Wang S, Liu Y, et al. Angle-shaped triboelectric nanogenerator for harvesting environmental wind energy. *Nano Energy* 2019;56: 269–76. <https://doi.org/10.1016/j.nanoen.2018.11.037>.
- [21] Wang C, Lai S-K, Wang J-M, Feng J-J, Ni Y-Q. An ultra-low-frequency, broadband and multi-stable tri-hybrid energy harvester for enabling the next-generation sustainable power. *Appl Energy* 2021;291:116825. <https://doi.org/10.1016/j.apenergy.2021.116825>.
- [22] Yang W, Gao Q, Xia X, Zhang X, Lu X, Yang S, et al. Travel switch integrated mechanical regulation triboelectric nanogenerator with linear-rotational motion transformation mechanism. *Extrem Mech Lett* 2020;37:100718. <https://doi.org/10.1016/j.eml.2020.100718>.
- [23] Wang Lu, He T, Zhang Z, Zhao L, Lee C, Luo G, et al. Self-sustained autonomous wireless sensing based on a hybridized TENG and PEG vibration mechanism. *Nano Energy* 2021;80:105555. <https://doi.org/10.1016/j.nanoen.2020.105555>.
- [24] Toyabur Rahman M, Sohel Rana SM, Salauddin Md, Maharjan P, Bhatta T, Kim H, et al. A highly miniaturized freestanding kinetic-impact-based non-resonant hybridized electromagnetic-triboelectric nanogenerator for human induced vibrations harvesting. *Appl Energy* 2020;279:115799. <https://doi.org/10.1016/j.apenergy.2020.115799>.
- [25] Yang W, Wang Y, Li Y, Wang J, Cheng T, Wang ZL. Integrated flywheel and spiral spring triboelectric nanogenerator for improving energy harvesting of intermittent excitations/trigging. *Nano Energy* 2019;66:104104. <https://doi.org/10.1016/j.nanoen.2019.104104>.
- [26] Lee DW, Jeong DG, Kim JH, Kim HS, Murillo G, Lee G-H, et al. Polarization-controlled PVDF-based hybrid nanogenerator for an effective vibrational energy harvesting from human foot. *Nano Energy* 2020;76:105066. <https://doi.org/10.1016/j.nanoen.2020.105066>.
- [27] Yuan M, Li C, Liu H, Xu Q, Xie Y. A 3D-printed acoustic triboelectric nanogenerator for quarter-wavelength acoustic energy harvesting and self-powered edge sensing. *Nano Energy* 2021;85:105962. <https://doi.org/10.1016/j.nanoen.2021.105962>.
- [28] Qiu W, Feng Y, Luo N, Chen S, Wang D. Sandwich-like sound-driven triboelectric nanogenerator for energy harvesting and electrochromic based on Cu foam. *Nano Energy* 2020;70:104543. <https://doi.org/10.1016/j.nanoen.2020.104543>.
- [29] Zi YL, Guo HY, Wen Z, Yeh MH, Hu CG, Wang ZL. Harvesting low-frequency (<5 Hz) irregular mechanical energy: a possible killer application of triboelectric nanogenerator. *ACS Nano* 2016;10:4797–805. <https://doi.org/10.1021/acsnano.6b01569>.
- [30] Zhang C, Tang W, Han C, Fan F, Wang ZL. Theoretical comparison, equivalent transformation, and conjunction operations of electromagnetic induction generator and triboelectric nanogenerator for harvesting mechanical energy. *Adv Mater* 2014;26(22):3580–91. <https://doi.org/10.1002/adma.v26.2210.1002/adma.201400207>.
- [31] Carneiro P, Soares dos Santos MP, Rodrigues A, Ferreira JAF, Simões JAO, Marques AT, et al. Electromagnetic energy harvesting using magnetic levitation architectures: a review. *Appl Energy* 2020;260:114191. <https://doi.org/10.1016/j.apenergy.2019.114191>.
- [32] Soares dos Santos MP, Ferreira JAF, Simões JAO, Pascoal R, Torráo J, Xue X, et al. Magnetic levitation-based electromagnetic energy harvesting: a semi-analytical non-linear model for energy transduction. *Sci Rep* 2016;6(1). <https://doi.org/10.1038/srep18579>.
- [33] Zhang B, Chen J, Jin L, Deng W, Zhang L, Zhang H, et al. Rotating-disk-based hybridized electromagnetic-triboelectric nanogenerator for sustainably powering wireless traffic volume sensors. *ACS Nano* 2016;10(6):6241–7. <https://doi.org/10.1021/acsnano.6b02384>.
- [34] Yang H, Deng M, Tang Q, He W, Hu C, Xi Yi, et al. A nonencapsulative pendulum-like paper-based hybrid nanogenerator for energy harvesting. *Adv Energy Mater* 2019;9(33):1901149. <https://doi.org/10.1002/aenm.v9.3310.1002/aenm.201901149>.
- [35] Archer CL, Jacobson MZ. Evaluation of global wind power. *J Geophys Res Atmos* 2005;110:D12110. <https://doi.org/10.1029/2004JD005462>.
- [36] Chen P, An J, Shu S, Cheng R, Nie J, Jiang T, et al. Super-durable, low-wear, and high-performance fur-brush triboelectric nanogenerator for wind and water energy harvesting for smart agriculture. *Adv Energy Mater* 2021;11(9):2003066. <https://doi.org/10.1002/aenm.v11.910.1002/aenm.202003066>.
- [37] Rahman MT, Rana S, Maharjan P, Salauddin Md, Bhatta T, Cho H, et al. Ultra-robust and broadband rotary hybridized nanogenerator for self-sustained smart-farming applications. *Nano Energy* 2021;85:105974. <https://doi.org/10.1016/j.nanoen.2021.105974>.
- [38] Ravichandran AN, Calmes C, Serres JR, Ramuz M, Blayac S. Compact and high performance wind actuated venturi triboelectric energy harvester. *Nano Energy* 2019;62:449–57. <https://doi.org/10.1016/j.nanoen.2019.05.053>.



**Xiang Li** was born in 1996 in Heilongjiang province, majored in mechanical engineering, and achieved the B.E. degree from the Shenyang University of Technology in 2018. Now, he is studying for a master's (M.S.) degree in mechanical engineering at Shenyang Jianzhu University. His research interest is environmental energy harvesting through triboelectric nanogenerators.



**Yuying Cao** received her M.Eng. degree in Control theory and control engineering from Yanshan University in 2016. She is currently a Ph.D. candidate in the Institute for Frontier Materials in Deakin University. Her research mainly focuses on triboelectric nanogenerator and sensors.



**Dr. Xin Yu** is a visiting scholar in Beijing Institute of Nano-energy and Nanosystems, Chinese Academy of Sciences, currently. He obtained the B.S. and Ph.D. degrees from College of Electronic Science and Engineering, Jilin University in 2009 and 2014, respectively. He was a visiting scholar in Department of Electrical and Computer Engineering, Michigan State University from 2017 to 2018. His interests are triboelectric nanogenerators, infrared gas sensing, and photoelectric detection.



**Yuhong Xu** was born in 1997 in Jilin province. She received her B.E. degree in automobile service engineering from the Jilin Engineering Normal University in 2019. She now is a graduate student in vehicle engineering at the Changchun University of Technology under the guidance of Professor Lu. Her research interest is triboelectric nanogenerators.



**Prof. Tinghai Cheng** received the B.S., M.S. and Ph.D. degrees from Harbin Institute of Technology in 2006, 2008 and 2013, respectively. He was a visiting scholar in the School of Materials Science and Engineering at Georgia Institute of Technology from 2017 to 2018. Currently, he is a professor of Beijing Institute of Nanoenergy and Nanosystems, Chinese Academy of Sciences. His research interests are triboelectric nanogenerators, piezoelectric energy harvester, and piezoelectric actuators.



**Yanfei Yang** was born in 1995 in Inner Mongolia Autonomous Region of China. He received his B.E. degree from Shenyang University of technology in 2018 and is now studying for a master's degree in mechanical engineering from Shenyang Jianzhu University. His research interest is triboelectric nanogenerator for energy harvesting.



**Prof. Zhong Lin Wang** received his Ph.D. from Arizona State University in physics. He now is the Hightower Chair in Materials Science and Engineering, Regents' Professor, Engineering Distinguished Professor and Director, Center for Nanostructure Characterization, at Georgia Tech. Dr. Wang has made original and innovative contributions to the synthesis, discovery, characterization and understanding of fundamental physical properties of oxide nanobelts and nanowires, as well as applications of nanowires in energy sciences, electronics, optoelectronics and biological science. His discovery and breakthroughs in developing nanogenerators established the principle and technological road map for harvesting mechanical energy from environment and biological systems for powering personal electronics. His research on self-powered nanosystems has inspired the worldwide effort in academia and industry for studying energy for micro-nano-systems, which is now a distinct disciplinary in energy research and future sensor networks. He coined and pioneered the field of piezotronics and piezophotonics by introducing piezoelectric potential gated charge transport process in fabricating new electronic and optoelectronic devices. Details can be found at: <http://www.nanoscience.gatech.edu>



**Dr. Shiming Liu** is an associate professor of the School of Mechanical Engineering, Shenyang Jianzhu University, Shenyang, China. He received his Ph.D. degree in mechanical design and theory from Harbin Institute of Technology, Harbin, China, in 2013. His research interests include mechanical system dynamics, mechanical structure stability and triboelectric nanogenerators.